JOURNAL OF GEOPHYSICAL RESEARCH, VOL. 101, NO. D19, PAGES 24,105–24,115, OCTOBER 30, 1996

Meteorological conditions associated with vertical distributions of aerosols off the west coast of Africa

Henry E. Fuelberg and Jonathan D. VanAusdall
Department of Meteorology, Florida State University, Tallahassee

Edward V. Browell
NASA Langley Research Center, Hampton, Virginia

Scott P. Longmore
Department of Meteorology, Florida State University, Tallahassee

Abstract. Vertical distributions of aerosol backscattering were obtained on Transport and Atmospheric Chemistry Near the Equator—Atlantic (TRACE A) flights parallel to the west coast of Africa using the airborne differential absorption lidar (DIAL) instrument. Aerosol distributions on the flight of October 15, 1992 (from 22°S to 5.5°S), exhibit strong horizontal and vertical gradients. The top of the aerosol layer ranges from 3.5 to 5.7 km above sea level, while its thickness ranges from 1.4 to 4.5 km. The greatest aerosol loading generally occurs near 4.0- to 4.5-km altitude between 8° and 12°S. Meteorological conditions are found to exert a major influence on the aerosol distributions. Dropsonde data along the flight track indicate numerous temperature inversions and stable layers in each sounding. The top of the aerosol region is associated with strong inversions due to subsidence. Five-day backward trajectories are calculated along the flight track at vertical intervals of 1 km using global meteorological analyses. Trajectories arriving at most locations of large aerosol loading originate over southern Africa, where biomass burning is occurring and deep surface-based mixed layers are common. Conversely, the air with less aerosol loading originates over the Atlantic Ocean. The exception is the northernmost segment of the flight above 3.5 km. Although this segment receives flow off Africa at these altitudes, lower level stable layers inhibit transport to higher levels. In addition, trajectories arriving at this part of the flight pass over a portion of Africa with reduced biomass burning and extensive deep convection that penetrates the stable layers.

1. Introduction

Numerous studies have examined aerosols over the tropical South Atlantic Ocean [e.g., *Chester et al.*, 1972; *Parkin et al.*, 1972; *Cachier et al.*, 1986; *Losno et al.*, 1992]. In a very recent paper, *Garstang et al.* [this issue] used satellite-derived measurements of aerosol optical depth to determine horizontal distributions of aerosols over the South Atlantic during August–October 1987 and 1992. The austral spring of 1992 coincided with the Southern African Fire-Atmosphere Research Initiative (SAFARI). They found enhanced aerosol loading extending into the Atlantic from the coasts of Angola and northern Namibia. In a related SAFARI study, *Swap et al.* [this issue] examined aerosol transport between southern Africa and the central South Atlantic Ocean (Ascension Island). West Africa, between 20°S and 10°N, was found to be the major source for air arriving in the lower troposphere over Ascension Island. The aerosols within this air were attributed largely to biomass burning and soil dust. In addition, air over southern Africa was found to undergo considerable recirculation due to closed anticyclones that are common over the region [*Garstang et al.*, this issue; *Swap et al.*, this issue].

Paper number 95JD02889.
0148-0227/96/95JD-02889$09.00

The Transport and Atmospheric Chemistry Near the Equator—Atlantic (TRACE A) experiment was conducted simultaneously with SAFARI. The TRACE A flights of October 14, 15, and 18 were conducted over the eastern South Atlantic Ocean, nearly parallel to the west coast of Africa [*Fishman et al.*, this issue]. These flights intersected the region of greatest aerosol loading described by *Garstang et al.* [this issue]. The airborne differential absorption lidar (DIAL) instrument [*Browell*, 1989, 1991] provided information about the vertical distribution of aerosol loading, while dropsondes released along the flight tracks yielded in situ meteorological data.

This paper examines meteorological conditions associated with aerosol distributions observed during the TRACE A flight of October 15, 1992. It complements *Garstang et al.* [this issue] and *Swap et al.* [this issue] by focusing on the vertical aerosol distribution between Africa and Ascension Island. Aerosol data from the DIAL are described first, followed by atmospheric thermodynamics revealed by the dropsonde data and land-based soundings. Backward trajectories then are used to estimate origins of the aerosol-laden air. Finally, trajectories for the October 15 case are compared with those for a month-long period during TRACE A.

2. Aerosol Distributions

The TRACE A flight of October 15, 1992, is depicted in Figure 1. The DC 8 aircraft departed Windhoek, Namibia

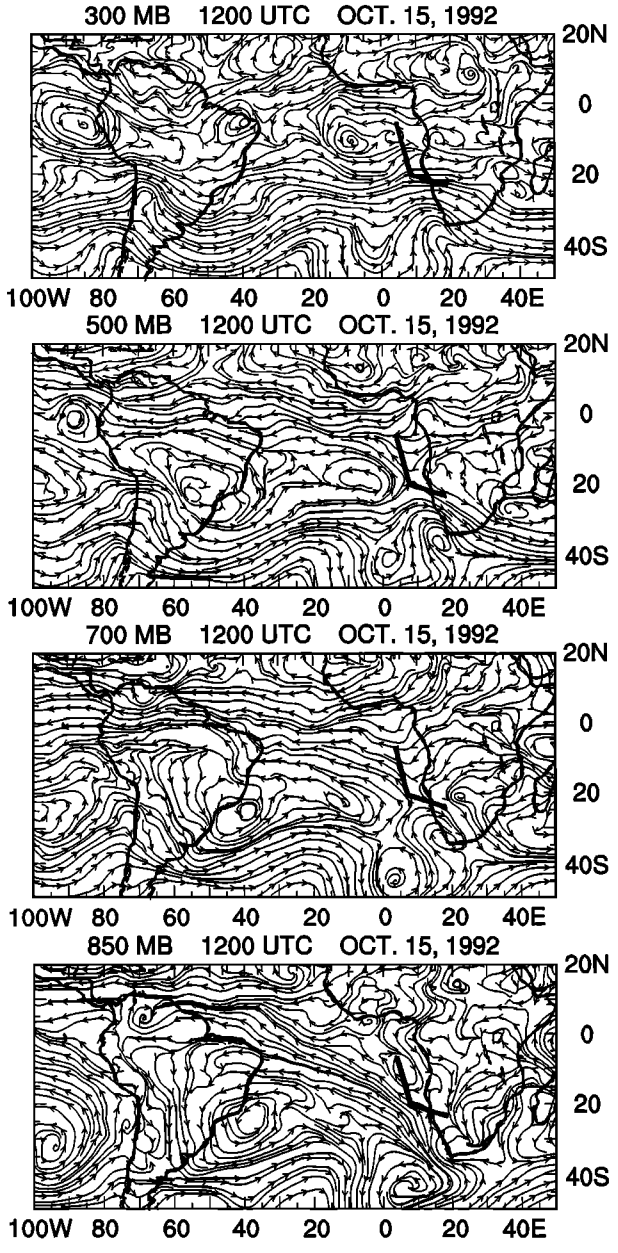

Figure 1. Streamline analyses from ECMWF data for various levels (in millibars) on 1200 UTC October 15, 1992. The flight track for October 15, 1992, is superimposed.

(22.5°S, 17.5°E), near 0720 UTC, headed northwest to near 20°S, 8°E, and then turned to a more northerly heading. The northernmost extent of the flight was 5.5°S, 4°E, and the aircraft cruising altitude was 10.2 km.

The airborne DIAL system has been used in many field experiments to study the distribution of aerosols and ozone in the troposphere and to relate these observations to chemical and dynamical processes [e.g., *Browell et al.*, 1988, 1990, 1994]. The lidar backscatter return at 1064 nm is used in the present analysis to determine the aerosol distribution along the DC 8 flight track during TRACE A. At this laser wavelength, the lidar return is most sensitive to aerosols with diameters greater than 1.0 μm [*Van de Hulst*, 1957]. This provides sensitivity to air masses with different amounts of large aerosols, such as is found in biomass burning plumes [*Andreae et al.*, 1988; *Anderson et al.*, this issue].

Aerosol distributions along the flight track exhibit strong horizontal and vertical gradients (Plate 1). For ease of presentation, we define the aerosol layer by values of relative atmospheric backscattering greater than 10 units (blue and green shades), and regions of heavy aerosol loading by values greater than 30 units (beginning with the yellow shading). Along the southern (left) portion of the flight, south of approximately 19°S, the aerosol layer is relatively thin and centered near 4 km. The aerosol loading is relatively light. The aerosol layer is thickest along the central portion of the flight, where its top reaches 5.7 km. Regions of heavy loading are found within this deepest region. Dark segments below ~1 km are due to extensive low-level cloud cover. The greatest relative aerosol backscattering, exceeding 50 units, occurs in a broad layer near 4-km altitude between 8° and 12°S. The top of the overall aerosol layer is gradually lower toward the north in this area. Finally, at the northernmost portion of the flight, the air is relatively free of aerosols at altitudes above 3.5 km; instead, greatest loading is near 1.5 km. The aerosol features on October 15 (Plate 1) are similar to those of the other flights in this area (October 14 and 18, not shown). The following sections examine meteorological conditions associated with the aerosol distributions of October 15.

3. Meteorological Conditions

Large-scale circulation patterns over the area are depicted using streamline analyses (Figure 1) obtained from the European Centre for Medium-Range Weather Forecasts (ECMWF) global data set [*Bengtsson*, 1985]. Flow patterns at all levels (850, 700, 500, and 300 mbar) exhibit strong horizontal and vertical shear along the flight. At 850 mbar (approximately 1.5 km above sea level) the flight passes through a weak cyclone located off the coast of Angola. At higher levels, important circulation features are the semipermanent anticyclone over the central South Atlantic Ocean, transient systems in the middle latitudes, and a col (a region of light and variable winds). The flight intersects the ridge line and col, with onshore flow along the southern reaches of the flight track but offshore flow in the northern portions. Additional information about flow patterns during TRACE A and SAFARI is given by *Bachmeier and Fuelberg* [this issue], *Diab et al.* [this issue], *Garstang et al.* [this issue], and *Swap et al.* [this issue].

Dropsondes were released at approximately 20-min intervals during the flight of October 15, for a total of seven soundings. These data describe in situ meteorological conditions along the flight track. Characteristics of the dropsonde data are outlined by the *National Center for Atmospheric Research* [1994]. Soundings from drops 1 (southernmost, 21°S, 11°E), 4 (central, 14°S, 6°E), and 7 (northernmost, 6°S, 4°E) are shown in Figure 2.

Numerous temperature inversions or stable layers are indicated along the flight track (Figure 2), but two features are most prominent. The well-known trade wind inversion is very intense; its base rises from approximately 0.9 km (915 mbar) at drop 1 to 1.2 km (880 mbar) at drop 7. These levels are approximately 0.5 km higher than annual values given by *von Ficker* [1936] and reported by *Garstang et al.* [this issue]. The inversion is deepest along the southern portion of the flight.

A second group of intense inversions occurs between 5.0 and 6.5 km (550 and 450 mbar) (Figure 2). Although present in all seven soundings, the inversion is most pronounced along the central portion of the flight (e.g., drop 4). It is highest along the northern end of the flight. These inversions are due to subsi-

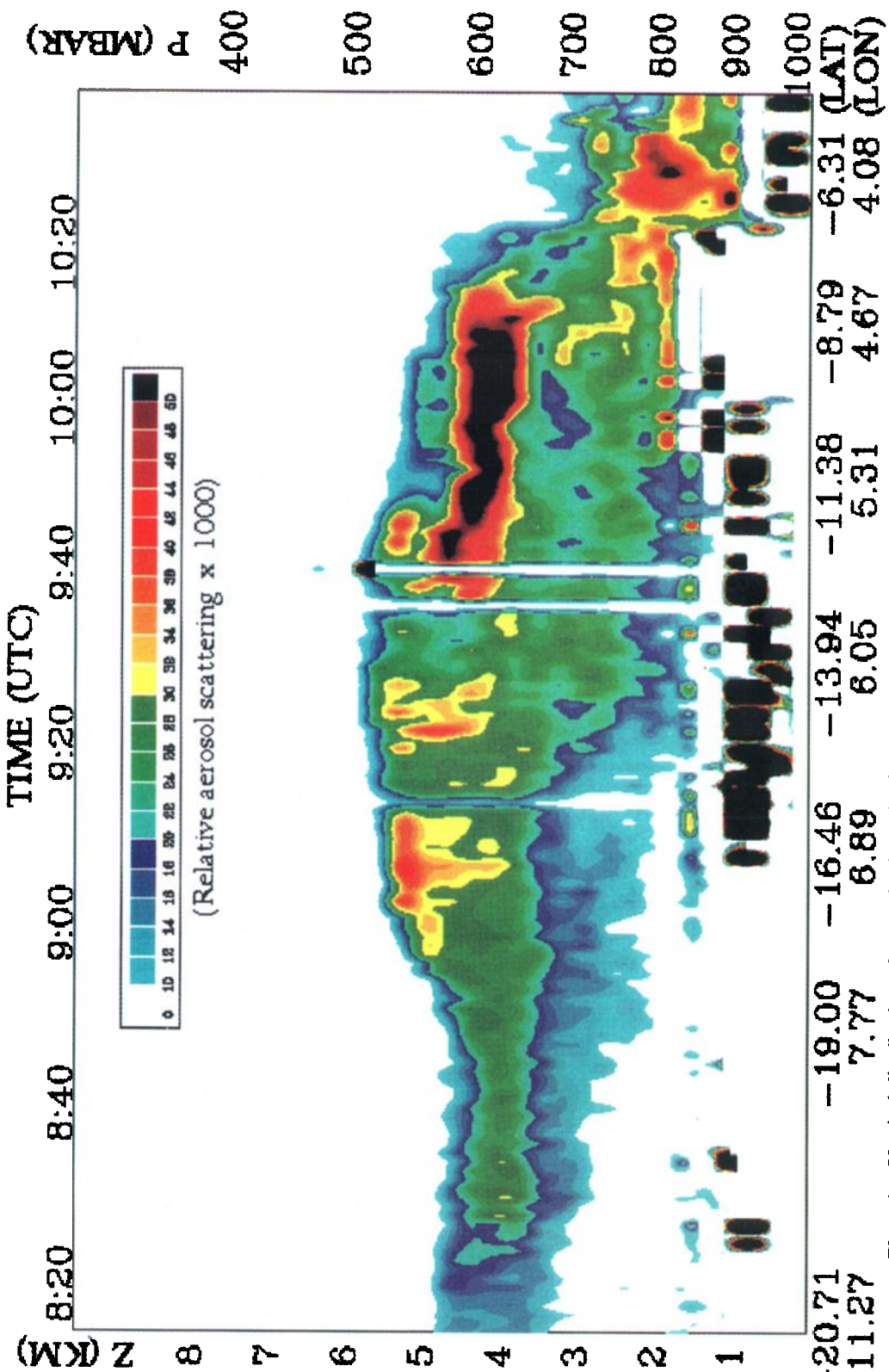

Plate 1. Vertical distribution of aerosols along the flight track of October 15, 1992, derived from the airborne DIAL instrument. The color scale denotes units of relative aerosol scattering ×1000. South is on the left side of diagram.

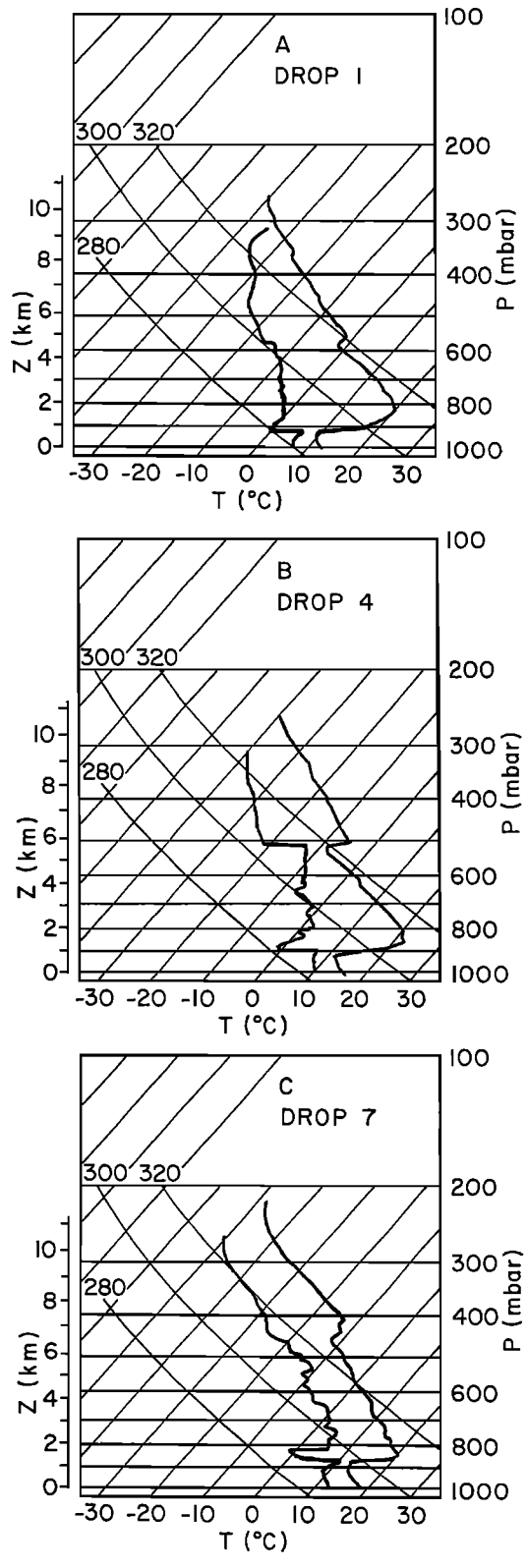

Figure 2. Skew T ln p diagrams of dropsonde data at locations (a) 1 (southernmost, 21°S, 11°E), (b) 4 (central, 14°S, 6°E), and (c) 7 (northernmost, 6°S, 4°E).

dence associated with the major anticyclone over the Atlantic. They are a semipermanent feature over southern Africa and Ascension Island during the TRACE A/SAFARI periods [*Garstang et al.*, this issue; *Swap et al.*, this issue].

We prepared a cross section showing the altitudes and strengths of all absolutely stable layers in the seven dropsonde-derived soundings (Figure 3a). The thickness of each bar represents the top and bottom of the stable layer, while its width corresponds to strength. The widest bars represent isothermal layers or temperature inversions in which potential temperature θ increases at a rate exceeding 10°C/km. The narrowest bars denote layers in which $\delta\theta/\delta z$ increases at between 5.0° and 7.5°C/km. These layers still are absolutely stable, since their temperature T lapse rates are less than the moist adiabatic value. Finally, an intermediate category denotes stable layers in which $\delta\theta/\delta z$ ranges between 7.5° and 10.0°C/km. Aerosol distributions are shown in the background (also see Plate 1).

The many stable/inversion layers along the flight track (Figure 3a) exhibit good spatial continuity. The trade wind inversion dominates the lowest 2 km of the cross section. The 2- to 5-km layer contains almost no stable layers along the southern two thirds of the flight. Conversely, the northernmost part of the flight, especially drop 7, contains several stable features within this layer. Multiple stable layers associated with subsidence are located above 5 km throughout the flight.

The top of the aerosol region corresponds to altitudes of major stable layers (Figure 3a). Many of the soundings exhibit several stable layers of various intensities above approximately 5 km; however, the top of the aerosol region generally agrees with the base of the lowest strong stable zone above the trade wind inversion. The aerosol region itself is almost free of stable layers. The northernmost location (drop 7) is especially interesting. Stable layers occur at lower altitudes than at locations farther south, and the top of the aerosol region is considerably lower as well (3.5 km). Nonetheless, the top of the enhanced aerosols coincides with a stable layer, albeit not the lowest one above the trade wind inversion. This is discussed further in the following sections.

Figure 3b contains an analysis of potential temperature along the flight track derived from the dropsonde data. Near the surface, the close vertical spacing of the isentropes denotes the very stable trade wind inversion. The subsidence inversions above 5 km are most intense near the center of the flight (e.g., drops 3 and 4). The bases of these inversions (Figures 2 and 3a) correspond to a potential temperature of approximately 320 K, and this value agrees closely with the top of the aerosol layer at all but the northernmost location (drop 7), where the top corresponds to a value near 317 K. The isentropes exhibit relatively large vertical spacing between 2 and 5 km along the southern two thirds of the flight. This denotes the nearly dry adiabatic lapse rates occurring in the layer (Figure 2). The wind data (Figure 3b) show the strong shears also seen in the ECMWF analyses (Figure 1).

Strong stable layers act as a cap or lid to synoptic-scale vertical motion. Thus there is little interaction between the layer near the surface (below the trade wind inversion) and the less stable air in the middle troposphere. Similarly, the intense subsidence inversions between 5 and 6 km greatly limit the exchange of air above and below it. Only intense convection would be able to penetrate these stable layers.

4. Trajectory Analyses

We determined the origins of air comprising the regions of large and small aerosol loading in Plate 1. Specifically, three-dimensional 5-day backward trajectories were calculated using a kinematic trajectory model in which parcels are advected by

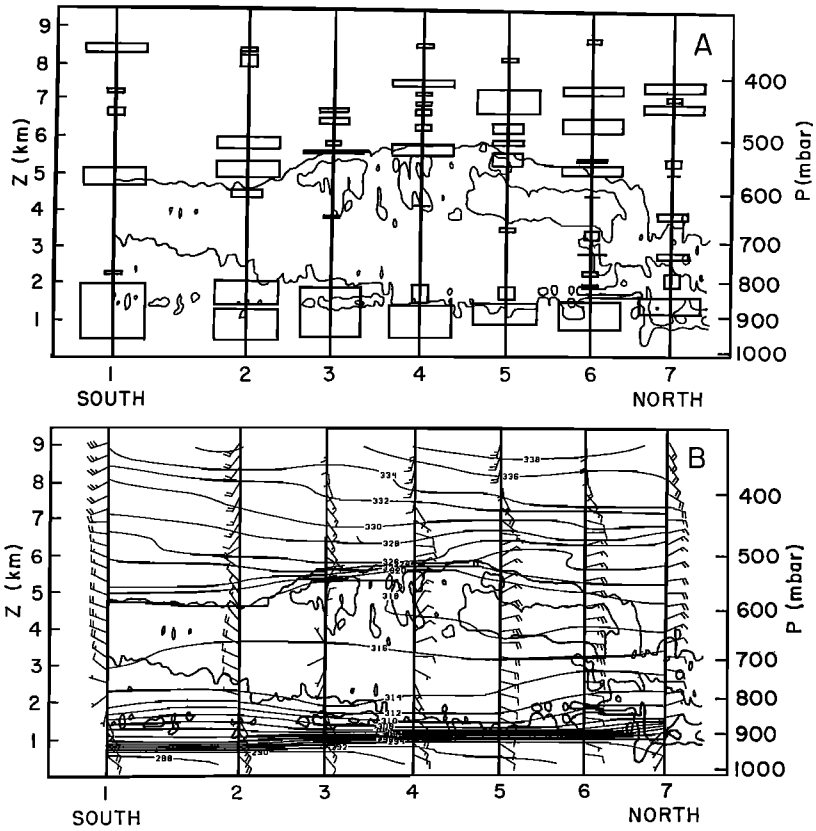

Figure 3. (a) Altitudes and strengths of major stable layers diagnosed from dropsonde data along the flight track. The width of each bar denotes the degree of stability, while the bar thicknesses denote the tops and bottoms of the stable layers. See text for additional details. Aerosol distributions from Plate 1 are superimposed, i.e., the 10- and 30-unit isolines. (b) Isentropes (in degrees Kelvin) and wind data along the flight track. Winds are in m s^{-1}, with short and long barbs denoting values of 2.5 and 5 m s^{-1}, respectively. Aerosol distributions are superimposed as in Figure 3a.

the winds without employing the isentropic assumption [*Fuelberg et al.*, this issue; *Loring et al.*, this issue]. ECMWF global analyses of the three wind components at 12-hour intervals between 1000 and 50 mbar served as input. *Pickering et al.* [this issue] noted that ECMWF analyses were marginally better than those from the National Meteorological Center during the TRACE A period. Nonetheless, the ECMWF wind analyses (Figure 1) do not agree perfectly with the observed dropsonde-derived winds (Figure 3b). This occurs because the regions of large horizontal and vertical shear are difficult to place accurately with the limited observations that are available over the South Atlantic Ocean.

Trajectories were calculated at 1-km vertical intervals between 1 and 9 km at each of the seven dropsonde release points. Acknowledging the large wind shears that are observed, and the uncertainties associated with the ECMWF analyses and trajectory methodologies, trajectories were obtained for clusters of points centered on each drop site. Similar procedures have been advocated by *Merrill et al.* [1985], *Kahl* [1993], and *Pickering et al.* [this issue]. Each cluster consisted of a 5 × 5 matrix of points, with each point separated by a 1° latitude/longitude interval. Thus a total of 1575 trajectories were prepared (7 drop sites × 9 levels × 25 points per cluster).

Since it is not feasible to show trajectories for all 63 clusters, we devised a simple procedure for quantifying the results and relating them to the aerosol distributions. Most aerosols arriving at Ascension Island (8°S, 14°W) during TRACE A/SAFARI were produced from vegetation, soils, and biomass burning over Africa [*Swap et al.*, this issue]. Therefore we counted the number of hours that the 25 trajectories of each cluster were over the African continent during the 5-day period. A trajectory cluster consisted of as many as 3025 hours (25 points × 121 hours); however, some trajectories arriving at 1 and 2 km intersected the surface before the end of the 5-day period. For example, one cluster arriving at 2 km consisted of as few as 2750 hours, while one arriving at 1 km had only 1736 hours. Figure 4 depicts the percentage of time that a cluster at each altitude was over the continent, i.e., actual hours divided by the number of possible hours (from 1736 to 3025 hours).

The above-mentioned procedure attempts to document the time that parcels spend over Africa; however, it has limitations. For example, the choice of a 5-day period was arbitrary. Most parcels that ultimately passed over Africa would do so within 2 or 3 days; however, some meandered over the water for longer periods before crossing the coastline. If trajectories had been calculated over 10-day periods, for example, the statistics in Figure 4 would change. These changes will be discussed in the following sections where appropriate.

The trajectory data (Figure 4) must be incorporated with the stability analyses (Figure 3) to understand the aerosol distributions (Plate 1). However, it is interesting that the trajectory data alone show generally good agreement with the vertical

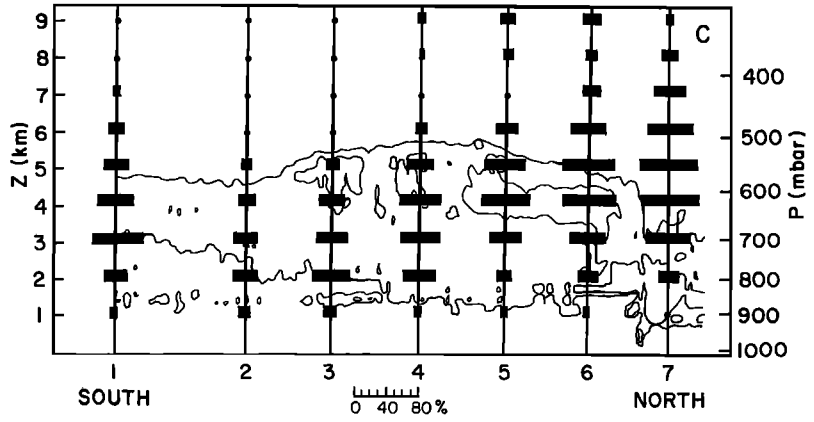

Figure 4. Percentages of time that a cluster spent over the African continent. See scale at the bottom. Values were obtained from trajectory analyses as described in the text. Aerosol distributions are superimposed as in Figure 3a.

distribution of aerosols (Figure 4). The northernmost drop site is the exception. In general, trajectories arriving at between 3- and 5-km altitude spend the greatest percentages of time over Africa, and this layer usually corresponds to the altitudes of largest aerosol loading (except for the extreme north). Conversely, the smallest percentages occur at 1 km and the top levels, where loadings are relatively small. Drop locations 1, 4, and 7 are examined in detail in the following paragraphs.

The air at 1 km (~905 mbar) is relatively free of aerosols at all locations along the flight track (Plate 1), and the trajectories reveal that this air has spent little time over Africa during the past 5 days (Figure 4). Percentages are less than 16% at all locations. Horizontal depictions of the trajectories show that air arriving at the southern end of the flight at 1 km (drop 1, Figure 5a) travels parallel to the coastline for several days before fanning out over the South Atlantic Ocean. At the northern end of the flight (drop 7, Figure 5c), the air arriving at 1 km originates farther north. More of these trajectories probably would reach central Africa if tracked beyond 5 days. Finally, parcels arriving near drop 4 originate from locations that are both farther north and south. The 1-km level is within the strong trade wind inversion (Figures 2 and 3a), and parcels arriving there experience only slight vertical displacement during the 5-day period (not shown).

Greatest aerosol loading along the southern two thirds of the flight occurs near 4 km. Trajectories arriving at 4 km (~635 mbar) within drop clusters 1 and 4 have spent approximately half of their 5-day histories over Africa (Figure 4). However, trajectory paths for these two drops differ considerably from each other (Figures 6a and 6b). All of the parcels arriving at cluster 4 originate almost due east over Africa. This area, between approximately 10° and 20°S, contains the greatest biomass burning during the TRACE A period [*Fishman et al.*, this issue]. Trajectories comprising cluster 1 originate over a much larger area. Many of them travel over the South Atlantic Ocean and follow long counterclockwise paths that pass over the southwestern corner of Africa. Others originate over Africa between 10° and 20°S. If the trajectory period were extended beyond 5 days, the percentages for cluster 4 would increase relative to those of cluster 1 (Figure 4), thereby agreeing with the greater aerosol loading at the more central site.

Time series of pressure altitudes for three trajectories arriving at 4 km (~635 mbar) in cluster 1 are shown in Figure 7a. Each of these parcels originates over south central Africa 5 days earlier (Figure 6a). They are typical of all the trajectories originating over this region. The parcels generally begin at lower levels, and their altitudes range from approximately 580 mbar (4.6 km) to 870 mbar (1.3 km) during the period. Corresponding time series for three representative trajectories arriving at 4 km in cluster 4 (Figure 7b) show a similar range of altitudes and similar origins at lower altitudes.

Few upper air sites are located over south central Africa; however, soundings are available at Etosha National Park, Namibia (19°S, 16°E), and Lusaka, Zambia (15°S, 28°E) (Figures 8a and 8b). These soundings exhibit a nearly dry adiabatic layer between the surface and 550–600 mbar (~4.5 km) that is capped by a temperature inversion. Deep mixed layers and associated capping inversions were common over southern Africa during TRACE A/SAFARI [*Garstang et al.*, this issue; *Swap et al.*, this issue]. Dry convective transport within such layers mixes surface-based aerosols throughout their depths. These soundings, the dropsonde data along the flight track (Figure 3a), and the altitude plots (Figures 7a and 7b) indicate that the trajectories originating over south central Africa remain within the mixed layer during their transits to clusters 1 and 4. This agrees with findings of *Swap et al.* [this issue] and *Garstang et al.* [this issue].

Unlike drop locations 1 and 4, location 7 at 6°S, 4°E is relatively free of aerosols at 4 km (Plate 1). Instead, the aerosol layer extends from about 1 to 3 km. This occurs even though parcels arriving at 4 and 5 km spend approximately 75% of their 5-day histories over Africa (Figure 4). A few of the 5-day trajectories originate north of the equator (Figure 6c); however, the majority begin between 0 and 10°S. Some factor other than African origin is responsible for the relatively aerosol free air above 3.5 km.

The sounding for drop 7 (Figure 2c) contains several stable layers below the top of the aerosol layer, i.e., between 2 and 4 km (Figure 3a). Trajectories indicate that air arriving at these levels (e.g., 4 km in Figure 6c) would have been over extreme western Africa approximately 2 days earlier, i.e., on October 13. Several conditions over western Africa might explain the relative aerosol minimum at location 7. The sounding at Brazzaville, Congo (4°S, 15°E), for 0948 UTC October 13 (Figure 8c) does not exhibit the deep surface-based mixed layer seen at Etosha and Lusaka (Figures 8a and 8b). Instead, it contains a

broad stable layer of varying intensity between approximately 1 and 3.0 km (900–700 mbar). This stable layer will inhibit aerosols from reaching higher levels. In addition, biomass burning was relatively infrequent north of approximately 10°S [*Fishman et al.*, this issue], and satellite imagery (not shown) indicates widespread deep convection over this portion of Africa on the days near October 15. The region of small aerosol loading

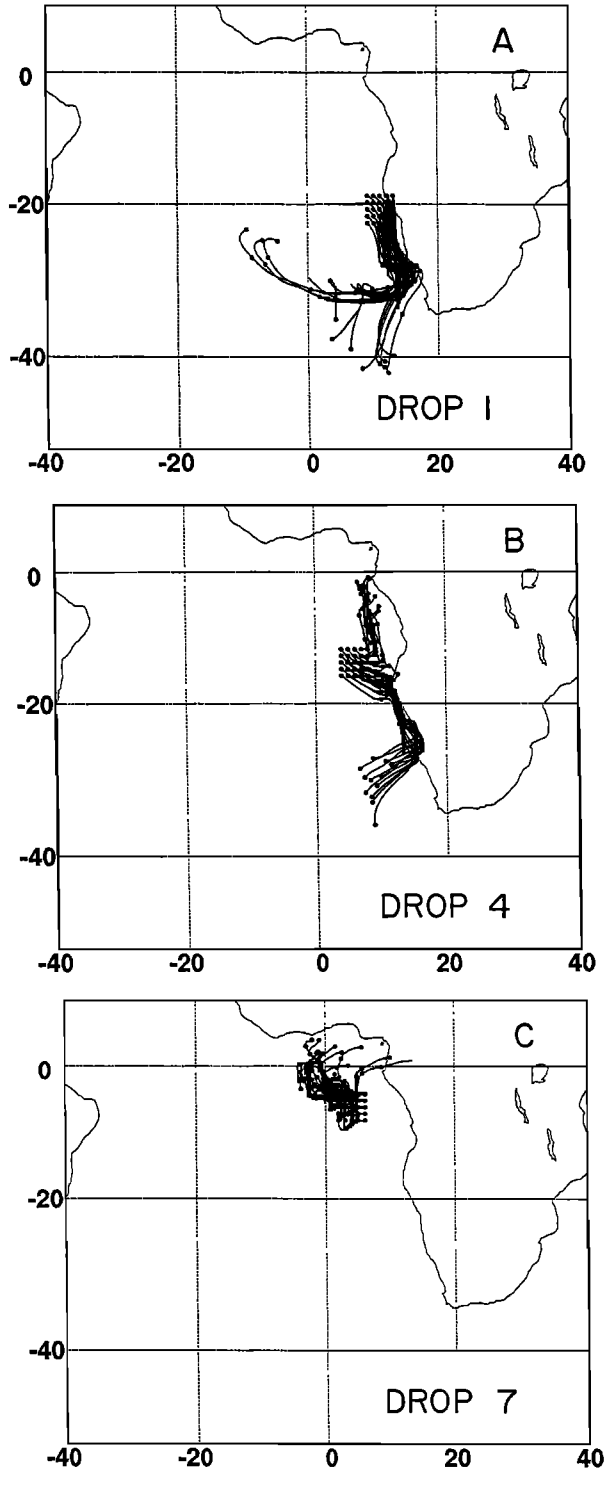

Figure 5. Horizontal depiction of 5-day backward trajectories arriving at 1 km (~905 mbar) for drop sites (a) 1, (b) 4, and (c) 7. Dots represent locations at 1-day intervals.

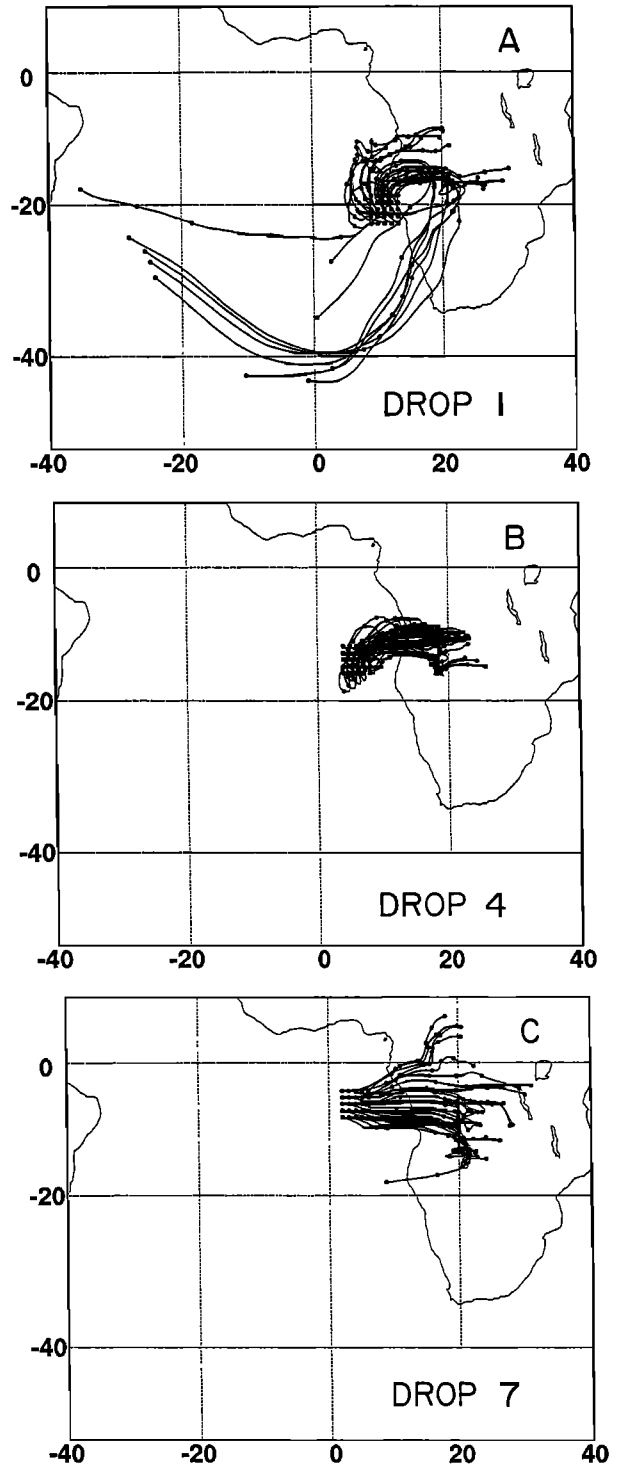

Figure 6. As in Figure 5, except for arrivals at 4 km (~635 mbar).

above 3.5 km corresponds to a wedge of enhanced ozone-rich air that is thought to have come from biomass burning over Africa [*Browell et al.*, this issue]. The lack of aerosols in the air mass possibly is due to removal by washout during convective transport. Pressure altitudes of selected trajectories arriving within cluster 7 at 4 km (Figure 7c) indicate that the air originates from a variety of altitudes. It is important to note that mesoscale motions associated with individual convective

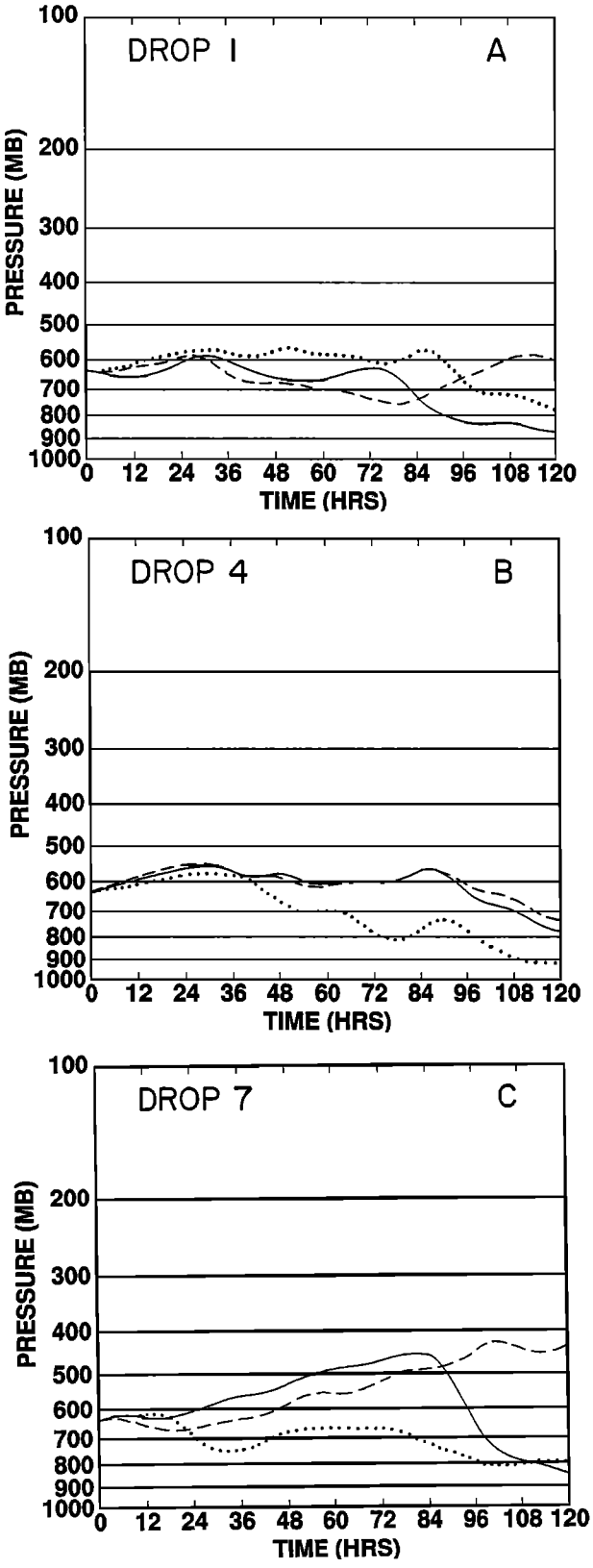

Figure 7. Time series of pressure altitude for selected trajectories arriving at 4 km (~635 mbar) in locations (a) 1, (b) 4, and (c) 7.

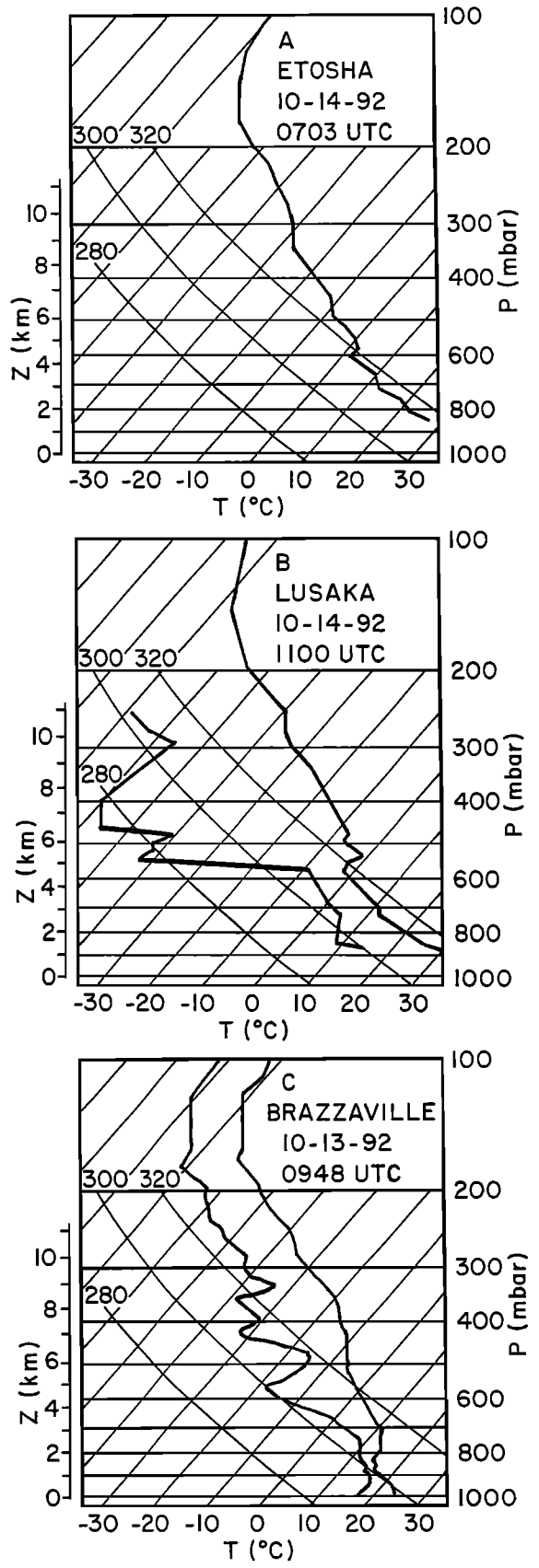

Figure 8. Skew T ln p diagrams for (a) Etosha National Park, Namibia (0703 UTC October 14, 1992), (b) Lusaka, Zambia (1100 UTC October 14, 1992), and (c) Brazzaville, Congo (0948 UTC October 13, 1992). No dew point data were available at Etosha.

storms are not resolved by the synoptic-scale ECMWF analyses. Thus trajectories passing through areas of deep convection are less likely to describe the motions actually experienced by air parcels.

The air at 7-km altitude is relatively free of aerosols at all locations along the flight track (Plate 1). At the five southernmost drop sites, the trajectories spend little time over Africa during the preceding 5 days (Figure 4). Instead, most begin over South America and the South Atlantic Ocean (e.g., drops 1 and 4 in Figures 9a and 9b). Furthermore, except for deep convective processes that can remove large aerosols, the aerosol-laden burning plumes that do originate over Africa are prevented from reaching this height by the strong stable layers at lower levels (Figure 3a). At the northernmost drop locations, air comprising the cluster spends more time over Africa (Figure 4), although many parcels still originate over the ocean (Figure 9c). As noted earlier, the numerous stable layers below 7 km will prevent aerosols from being transported to this higher altitude, and the deep convection north of 10°S probably reduces their concentration as well.

5. Generality of Findings

It is important to consider the generality of current findings. Enhanced aerosol loading off the coasts of Angola and northern Namibia appears to be common during austral spring

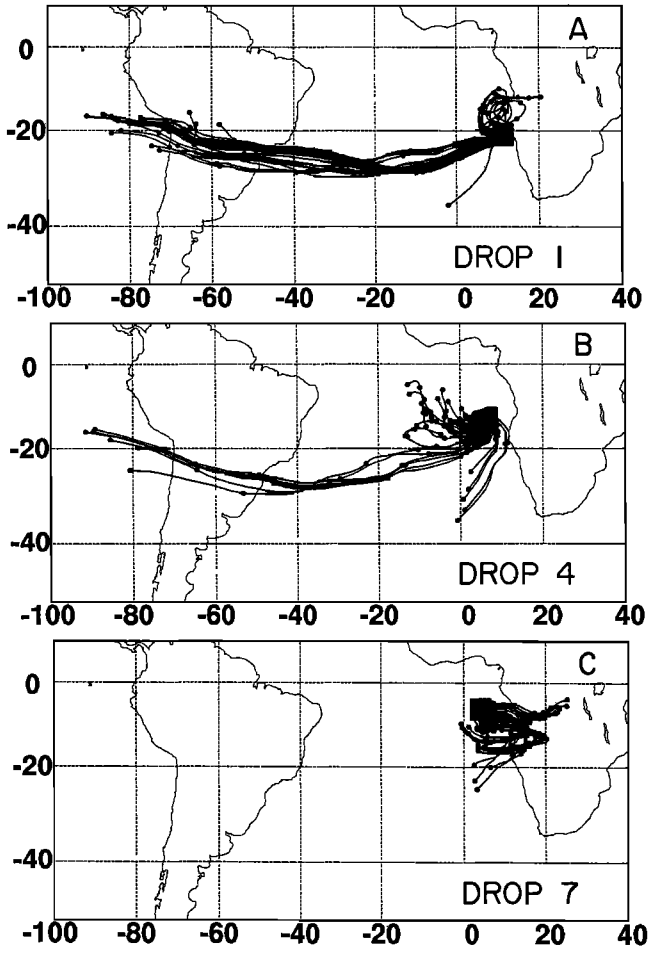

Figure 9. As in Figure 5, except for arrivals at 7 km (~435 mbar).

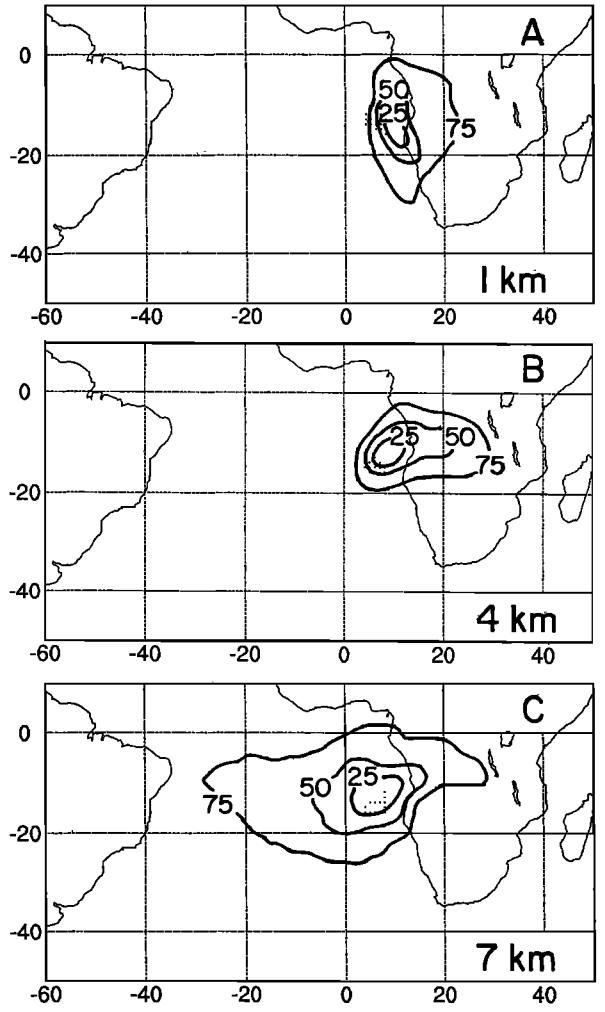

Figure 10. Percentages of trajectory hours for daily arrivals between September 27 and October 26, 1992. Calculations were made for grid squares of 1° latitude/longitude; 25% of residence time hours are contained within each contoured region. The 5-day backward trajectories arrive at the 5 × 5 cluster of points at altitudes of (a) 1 km, (b) 4 km, and (c) 7 km.

[*Garstang et al.*, this issue]. The vertical distributions of these aerosols were quite similar on October 14, 15, and 18 (not shown). In addition, the trade wind temperature inversion near 1 km and the intense subsidence inversions between 5 and 6 km are semipermanent features of the region [*Garstang et al.*, this issue; *Swap et al.*, this issue].

We examined the generality of trajectories ending on October 15 by calculating additional trajectories ending on each day between September 27 and October 26, 1992, i.e., encompassing most of the TRACE A period. The methodologies used here were similar to those described in section 4. To facilitate the display of results, procedures similar to those of *Poirot and Wishinski* [1986] and *Merrill* [1994] were employed. Specifically, we counted the number of hours spent by the trajectories within grid boxes of 1° latitude/longitude. Figure 10 shows results for trajectories arriving at site 4 at altitudes of 1, 4, and 7 km. The isopleths denote percentages of the total number of trajectory hours. That is, each isoline encompasses 25% of the total number of hours. We did not apply the geometrical cor-

rection factor utilized by *Poirot and Wishinski* [1986] and *Merrill* [1994].

Results for the month-long period generally are similar to those of October 15. Iscpleths for arrivals at 1 km (Figure 10a) are elongated along the coastline; however, many trajectories do pass over southern Africa. This was not observed on October 15 (Figure 5b). One should recall that trajectories were terminated once they intersected the surface. Most 4-km arrivals for the month-long period have passed over south central Africa (Figure 10b), and this is very similar to the situation on October 15 (Figure 6b). Finally, many of the arrivals at 7 km (Figure 10c) have resided over the South Atlantic Ocean, similar to findings of the current case (Figure 9b). One should note, however, that some air parcels from Africa do reach site 4 at 7 km (note the elongation of the 75% isopleth). This only occurred at locations farther north on October 15 (Figure 9c).

6. Summary and Conclusions

The TRACE A flight of October 15, 1992, was just off the west coast of southern Africa from 22.5°S to 5.5°S. This is a region of large aerosol loading [e.g., *Garstang et al.*, this issue]. The airborne DIAL instrument indicated major variations in the vertical distribution of aerosols. The top of the aerosol layer ranged from 3.5 to 5.7 km, while its thickness ranged from 1.4 to 4.5 km. Greatest aerosol loading generally occurred near 4.0- to 4.5-km altitude between 8° and 12°S, where the aerosol layer was thickest.

Meteorological conditions and air parcel trajectories were closely associated with the aerosol distributions. Dropsonde data indicated that the southern two thirds of the flight contained strong subsidence-induced inversions or stable layers above approximately 5 km. Although multiple stable layers often were present above 5 km, the top of the aerosol region corresponded to the altitude of the lowest one. This is expected, since stable layers inhibit vertical transport. The depth of the aerosol region coincided with a layer of near-neutral stability.

Trajectory analyses showed that the southern two thirds of the aerosol region consisted of parcels that had spent considerable time over the African continent, where a deep surface-based mixed layer was prevalent. Altitudes of these parcels were consistent with those of the stable layers. The relatively aerosol free air above and below the aerosol layer originated over the South Atlantic Ocean.

The top of the aerosol region was much lower over the northernmost portion of the flight (approximately 3.5 km) than over locations further south. Although air above this top still originated over Africa and contained enhanced ozone, stable layers in the lower troposphere apparently prevented the aerosols from being transported to the higher levels. These lower level stable layers were not present further south. In addition, most trajectories arriving at altitudes above 3.5 km originated over a part of Africa (north of 10°S) where biomass burning was less frequent [*Fishman et al.*, this issue] and which contained extensive deep convection.

In conclusion, aerosol loading off the west coast of Africa exhibits strong horizontal and vertical gradients. The transport of this aerosol-laden air from Africa is heavily influenced by atmospheric stability. Furthermore, since flow patterns over the region are complex, trajectories for nearby points can vary greatly. The results for October 15, 1992, appear to be representative of austral spring. However, additional aerosol observations, sounding data, and trajectory calculations will be necessary to confirm this hypothesis. It is clear that the combination of DIAL observations and meteorological analyses is a powerful tool for understanding aerosol distributions and their transport.

Acknowledgments. This research was sponsored by NASA under grant NAG1-1312 from the Tropospheric Chemistry Program. We appreciate the assistance of Jim Hoell and Jack Fishman of NASA Langley Research Center (LaRC), and Scott Bachmeier at Lockheed/LaRC. Rob Loring and Mark Watson at FSU also were very helpful. The dropsonde data were provided by Dean Lauritsen of the National Center for Atmospheric Research. The soundings at Etosha were under the supervision of Roseanne Diab of the Univeristy of Natal–Durban. The soundings at Brazzaville were collected by Dominique Nganga.

References

Anderson, B. E., W. B. Grant, G. L. Gregory, E. V. Browell, J. E. Collins Jr., G. W. Sachse, D. R. Bagwell, and C. H. Hudgins, Aerosols from biomass burning over the tropical South Atlantic region: Distributions and impacts, *J. Geophys. Res.*, this issue.

Andreae, M. O., et al., Biomass burning emissions and associated haze layers over Amazonia, *J. Geophys. Res.*, *93*, 1509–1527, 1988.

Bachmeier, S. A., and H. E. Fuelberg, A meteorological overview of the Transport and Atmospheric Chemistry Near the Equator–Atlantic (TRACE A) period, *J. Geophys. Res.*, this issue.

Bengtsson, L., Medium-range forecasting—The experience of ECMWF, *Bull. Am. Meteorol. Soc.*, *66*, 1133–1146, 1985.

Browell, E. V., Differential absorption lidar sensing of ozone, *Proc. IEEE*, *77*, 419–432, 1989.

Browell, E. V., Ozone and aerosol measurements with an airborne lidar system, *Opt. Photonics News*, 8–11, 1991.

Browell, E. V., G. L. Gregory, R. C. Harriss, and V. W. J. H. Kirchoff, Tropospheric ozone and aerosol distributions across the Amazon Basin, *J. Geophys. Res.*, *93*, 1431–1451, 1988.

Browell, E. V., G. L. Gregory, R. C. Harriss, and V. W. J. H. Kirchoff, Ozone and aerosol distributions over the Amazon Basin during the wet season, *J. Geophys. Res.*, *95*, 16,887–16,901, 1990.

Browell, E. V., M. A. Fenn, C. F. Butler, W. B. Grant, R. C. Harriss, and M. C. Shipham, Ozone and aerosol distributions in the summertime troposphere over Canada, *J. Geophys. Res.*, *99*, 1739–1755, 1994.

Browell, E. V., et al., Ozone and aerosol distributions and air mass characteristics over the South Atlantic basin during the burning season, *J. Geophys. Res.*, this issue.

Cachier, H., P. Buat-Menard, M. Fontugne, and P. Chesselet, Long-range transport of continentally derived particulate carbon in the marine atmosphere: Evidence from stable carbon isotope studies, *Tellus*, *38*, 161–177, 1986.

Chester, R., H. Elderfield, J. J. Griffin, L. R. Johnson, and R. C. Padgham, Eolian dust along the eastern margins of the Atlantic Ocean, *Mar. Geol.*, *13*, 91–105, 1972.

Diab, R. D., M. R. Jury, J. M. Combrink, and F. Sokolic, A comparison of anticyclone and trough influences on the vertical distribution of ozone and meteorological conditions during SAFARI 92, *J. Geophys. Res.*, this issue.

Fishman, J., J. M. Hoell Jr., R. D. Bendura, V. W. J. H. Kirchoff, and R. J. McNeal Jr., NASA GTE TRACE A experiment (September–October 1992): Overview, *J. Geophys. Res.*, this issue.

Fuelberg, H. E., R. O. Loring Jr., M. V. Watson, M. C. Sinha, K. E. Pickering, A. M. Thompson, G. W. Sachse, D. R. Blake, and M. R. Schoeberl, TRACE A trajectory intercomparison, 2, Isentropic and kinematic methods, *J. Geophys. Res.*, this issue.

Garstang, M., P. D. Tyson, R. Swap, M. Edwards, P. Kallberg, and J. A. Lindesay, Horizontal and vertical transport of air over southern Africa, *J. Geophys. Res.*, this issue.

Kahl, J. D., A cautionary note on the use of air trajectories in interpreting atmospheric chemistry measurements, *Atmos. Environ.*, 27A, 3037–3038, 1993.

Loring, R. O., Jr., H. E. Fuelberg, J. Fishman, M. V. Watson, and E. V. Browell, Influence of a middle-latitude cyclone on tropospheric

ozone distributions during a period of TRACE A, *J. Geophys. Res.*, this issue.

Losno, R., G. Bergametti, and P. Carlier, Origins of atmospheric particulate matter over the North Sea and the Atlantic Ocean, *J. Atmos. Chem.*, *15*, 333–352, 1992.

Merrill, J. T., Isentropic airflow probability analysis, *J. Geophys. Res.*, *99*, 25,881–25,889, 1994.

Merrill, J. T., R. Bleck, and L. Avila, Modeling atmospheric transport to the Marshall Islands, *J. Geophys. Res.*, *90*, 12,927–12,936, 1985.

National Center for Atmospheric Research, SSSF observing facilities: Description and specifications, Version 1.0, Surface and Sounding Syst. Facility, Boulder, Colo., 1994.

Parkin, D. W., D. R. Phillips, R. A. L. Sullivan, and L. R. Johnson, Airborne dust collections down the Atlantic, *Q. J. R. Meteorol. Soc.*, *98*, 798–808, 1972.

Pickering, K. E., A. M. Thompson, D. P. McNamara, M. R. Schoeberl, H. E. Fuelberg, R. O. Loring Jr., M. V. Watson, K. Fakhruzzaman, and A. S. Bachmeier, TRACE A trajectory intercomparison, 1, Effects of different input analyses, *J. Geophys. Res.*, this issue.

Poirot, R. L., and P. R. Wishinski, Visibility, sulfate and air mass history associated with the summertime aerosol in northern Vermont, *Atmos. Environ.*, *20*, 1457–1469, 1986.

Swap, R., M. Garstang, S. A. Macko, P. D. Tyson, W. Maenhaut, P. Artaxo, P. Kallberg, and R. Talbot, The long-range transport of southern African aerosols to the tropical south Atlantic, *J. Geophys. Res.*, this issue.

Van de Hulst, H. C., *Light Scattering by Small Particles*, John Wiley, New York, 1957.

von Ficker, H., Die passatinversion, *Veroffenlichungen Meteorol. Inst. Univ. Berlin*, *1*, 33 pp., 1936.

E. V. Browell, NASA Langley Research Center, Hampton, VA 23681.

H. E. Fuelberg, S. P. Longmore, and J. D. VanAusdall, Department of Meteorology, Florida State University, Tallahassee, FL 32306-3034. (e-mail:fuelberg@met.fsu.edu)

(Received March 21, 1995; revised July 24, 1995;
accepted July 24, 1995.)